Cryogenic mechanical loss of amorphous germania and titania-doped germania thin films

S Khadka[1], A Markosyan[1], K Prasai[1], A Dana[1], L Yang[2], S C Tait[3], I W Martin[3], C S Menoni[2], M M Fejer[1] and R Bassiri[1]

[1] E. L. Ginzton Laboratory, Stanford University, Stanford, California 94305, USA
[2] Department of Electrical and Computer Engineering, Colorado State University, Fort Collins, Colorado 80523, USA
[3] SUPA, School of Physics and Astronomy, University of Glasgow, Glasgow G12 8QQ, United Kingdom

E-mail: khadka@stanford.edu

Abstract. The mechanical loss of amorphous thin films of germania (GeO_2) and titania-doped germania (Ti:GeO_2) deposited by ion-beam sputtering onto silicon double-paddle oscillators was studied from 10 K to 290 K. Undoped germania was found to show a wide cryogenic mechanical loss peak centered at $\sim$ 60 K with $\phi = 3.1 \times 10^{-3}$, which decreases to 1.1×10^{-3} as Ti-concentration increases to 44%. In addition to decreasing the height of this low-temperature peak, Ti-doping increases its width, and shifts its position towards lower temperatures. Annealing reduces the room temperature mechanical loss of Ti:GeO_2 and increases its cryogenic mechanical loss, which is consistent with trends observed in most amorphous oxides.

1. Introduction

The mirror coatings used in precision optical measurement instruments such as gravitational wave detectors (GWD) are typically dielectric coatings consisting of alternating layers of high- and low-refractive index amorphous oxides. These coatings must meet a stringent set of optical requirements including low scatter and absorption losses, and, in order to reduce their contribution to thermal displacement noise, low mechanical losses as well. The mechanical loss of amorphous films is known to depend on film compositions, growth conditions, and annealing. The current generation of LIGO [1] and Virgo [2] GWDs use ion-beam sputtered (IBS) silica (SiO_2) as the low index material and titania-doped tantala (Ti:Ta_2O_5) as the high-index material. In the current Advanced LIGO mirrors, for example, the mechanical loss measured on single layers of SiO_2 films is 4×10^{-5} while that of 25% Ti:Ta_2O_5 is 2.4×10^{-4} [3–5] indicating that the high-index layer is the dominant contributor to coating thermal noise. Efforts to reduce coating mechanical loss, and therefore thermal noise, have been focused on developing new materials to replace the high-index layers.

Recent investigations have shown that GeO_2-based films are one of the promising materials for room temperature GWDs, as the measured mechanical loss of undoped GeO_2 films at room temperature is significantly lower than that of any other known amorphous oxides other than SiO_2 [6, 7]. Thus, a solution currently under investigation is to replace the current Ti:Ta_2O_5 with GeO_2-based layers. With SiO_2 used as the low-index layer ($n = 1.45$ at 1064 nm wavelength), it is necessary to increase the refractive index of GeO_2 ($n = 1.65$) with suitable dopants [5, 6] to reduce the number of layer pairs for the required reflectivity

to a point where lower total mechanical loss of the multi-layer films can be realized. Coatings of SiO_2 and 44% Ti:GeO_2 ($n = 1.88$) films are predicted, based on mechanical loss measurements on single layers, to lower the room-temperature thermal noise to half the value of the current Advanced LIGO coatings, which would meet the design target for Advanced LIGO + [6].

To enhance the performance of future generations of GWDs that may also operate at low temperatures, such as LIGO Voyager [8] and Einstein Telescope [9], it is crucial to investigate the characteristics and mechanisms of mechanical loss not only at room temperature but also at cryogenic temperatures. Previous studies on SiO_2 and Ta_2O_5-based coatings have demonstrated temperature-dependent mechanical losses, exhibiting distinct patterns at low temperatures, such as peaks that increase upon post-deposition annealing [10, 11] or are suppressed with the addition of dopants [12].

The temperature-dependent mechanical loss observed in bulk and thin-film samples has been analyzed in terms of the distribution of two-level systems (TLS) of various barrier heights, asymmetries, etc [11]. The examination of low-temperature loss in these coatings has facilitated insights into the nature of TLS by measuring barrier height distributions [11] or by directly modeling mechanical loss from TLS calculations based on atomic structure models [13, 14]. Consequently, it is useful to measure mechanical loss as a function of temperature to further investigate and comprehend the TLS mechanism for mechanical loss. These measurements will also enable the evaluation of these materials' suitability for potential use in future cryogenic GWDs.

Although GeO_2-based films have emerged as one of the promising candidates for the mirror coatings for Advanced LIGO +, they are much less studied than their counterpart SiO_2 at lower temperatures. Earlier studies have drawn many parallels between the properties of SiO_2 and GeO_2 [15]. Structurally, GeO_2 and SiO_2 glasses are similar to each other: both have tetrahedral building blocks with corner sharing (CS), and few edge- and face-sharing connections (ES and FS, respectively). The latter types of polyhedral connections are empirically shown to correlate with higher mechanical loss at room temperature [16]. While data are available for the temperature-dependent losses in bulk GeO_2 [17], no temperature-dependent data are available for the mechanical loss of GeO_2 thin films. In addition when GeO_2 is co-sputtered with high-index oxides as is necessary for the LIGO coating design, the mechanical loss is expected to exhibit a complex dependence on composition, as does the atomic structure of mixed films [5, 7]. In order to further reduce the mechanical loss, the films are subjected to post-deposition heat treatment at temperatures below their crystallization point. The way in which the temperature-dependent mechanical loss of these GeO_2 based thin films evolves at various annealing temperatures is also not well understood.

In this work, we report the measurements of mechanical loss of ion-beam sputtered GeO_2 and Ti:GeO_2 thin films as a function of temperature from 10 K to 290 K. The mechanical loss values are evaluated from ring-down measurements from double-paddle oscillators (DPO) on which the respective thin films were deposited. We report significant trends in mechanical loss as a function of TiO_2 concentration as well as annealing conditions. We compare the results from our measurements from a thin film of GeO_2 with the literature results from bulk GeO_2. The purpose of these measurements is to provide data useful for comparison with predictions from atomic models of amorphous Ti:GeO_2, enabling the study of TLS in these materials. In addition, understanding how one can reduce the mechanical loss in these coatings will aid in the design and optimization for future GWDs.

2. Experimental methods

2.1. Cryogenic measurement of mechanical loss

The mechanical loss of coatings used in the LIGO optics are usually measured by "ring-down" experiments using electrostatically actuated mechanical resonators. There are two well-established techniques to hold the resonators: The first is a system where the mechanical resonator, such as a cantilever or DPO, made of crystalline silicon is clamped in the measurement system [18, 19], and the second is a gentle nodal suspension system (GeNS) where the resonator is a thin disc balanced on a spherical support [20, 21]. Here, we use a silicon DPO resonator clamped in between two slabs of invar that form the sample holder, and secured using two identical screws. A digital torque wrench is used while tightening the clamp, ensuring the same torque is applied on both screws. The sample holder is mounted onto the cold finger inside the cryostat. The DPO has a single low mechanical loss anti-symmetric mode (see section 2.2) which is isolated from the clamp, as described in [22]. The experimental setup for the measurements is similar to that of reported in [22, 23]. Figure 1 shows the schematic of a flow cryostat with a sample unit, that holds the clamp for the resonator, attached to the base of its cold finger. There are three silicon diode temperature sensors (TS) installed at different positions inside the cryostat; TS1 is placed nearest to the base of cold finger controls and maintains a constant temperature inside the cryostat, TS2 is placed at the clamp and measures the temperature at the closest spot to the resonator, and TS3 is placed at the end of the sample holder in order monitor the temperature distribution within the sample unit. Instead of the electrical read-out system used conventionally with DPOs, we implemented an optical read-out system based on a super-luminescent diode (SLD) and a split photo-diode to detect the amplitude of the beam deflection. The system operates at 1.5 µm wavelength, which mitigates heat accumulation due to absorption from the silicon-based DPO. In addition, the utilization of a broadband light source precludes potential interference originating from the DPO's front and back surfaces.

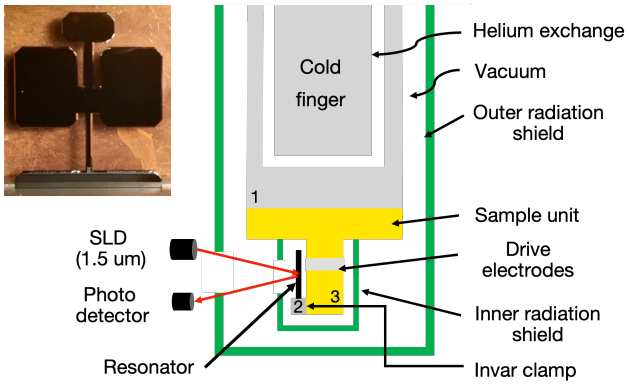

Figure 1. Schematic of the flow cryostat used for the mechanical loss measurement of thin films. Silicon thermal sensors (TS) TS1, TS2 and TS3 are placed in the position 1, 2, and 3, respectively. Inset image shows a DPO mounted in the clamp attached to the cold finger of the cryostat.

2.2. Silicon resonators

The DPO, as shown in the inset of figure 1, comprises of a head, neck, two wings, leg and foot, where the neck and head make one oscillator and two wings make the other [22, 24]. Among the nine modes of a DPO, that can be measured within 10 kHz, the second anti symmetric

torsional mode (AS2), at $\sim$5.65 kHz, has a low mechanical loss on the order of 1×10^{-7} below 150 K. In the AS2 mode, the two oscillators of the DPO move out of phase, twisting the neck, in addition to the out-of-phase movement of the two wings about the central axis. Hence, during this oscillation, the majority of strain energy is stored in the neck region while the clamped region at the foot ideally is motionless, isolating the AS2 mode from reaction damping and clamping loss [25].

The DPOs were fabricated from high quality float-zone silicon wafers coated with silicon nitride (SiN) at the Stanford Nanofabrication Facility (SNF) using the process described in [26]. The photolithographic pattern was transferred from the resist to the SiN layer with reactive-ion etching. Then the patterned wafer with SiN as the etch mask was dipped in a bath of potassium hydroxide (KOH) solution at 80°C to release individual DPOs coated with SiN. Finally, the SiN layers on each of DPOs were wet etched, using 25% hydrofluoric (HF) acid, which leaves the DPO surface hydrophobic. In order to minimize any changes in the mechanical loss of the silicon resonators resulting from post-deposition annealing of the coatings under investigation, the fabricated DPOs were pre-annealed at 600°C for 6 hrs prior to deposition of the coating.

2.3. Mechanical loss measurement and data reduction

The mechanical loss of the thin films was evaluated using "ring-down" measurements, which involves excitation of a mode in a resonator, and reading the decaying amplitude of the mode as it continues its free vibration. The amplitude of such decaying oscillation in the absence of external forces is expressed as $A(t) = A_0 e^{-t/\tau}$, with the mechanical loss angle given by $\phi = 1/(\pi f \tau)$, where τ is the decay constant extracted from the exponential fitting of the decaying amplitude curve, and f is the frequency of the resonant mode. The mechanical loss is the ratio of elastic energy loss per cycle ΔE to the total elastic energy of the oscillation E,

$$\phi = \frac{\Delta E}{2\pi E}. \tag{1}$$

For a 300-µm-thick DPO coated with a $\sim$500-nm-thick coating, the energy in the substrate ($E_{\rm sub}$) is significantly larger than the energy in the thin film ($E_{\rm film}$). Therefore, for a coated DPO equation 1 can be expressed as [23],

$$\phi_{\rm coated} = \phi_{\rm uncoated} + \frac{E_{\rm film}}{E_{\rm sub}}\phi_{\rm film}, \tag{2}$$

where $\phi_{\rm coated}$ is the mechanical loss of a coated DPO, $\phi_{\rm uncoated}$ is that of a bare or uncoated DPO, and $\phi_{\rm film}$ is the mechanical loss of the coating.

For the torsional mode of the DPO, the energy ratio in equation 2 is given as [23]

$$\frac{E_{\rm film}}{E_{\rm sub}} = \frac{3G_{\rm film}t_{\rm film}}{G_{\rm sub}t_{\rm sub}}, \tag{3}$$

where $G_{\rm sub}$ and $G_{\rm film}$ are the shear moduli and $t_{\rm sub}$ and $t_{\rm film}$ are thicknesses of the Si-substrate and thin film, respectively. Combining equations 2 and 3 the mechanical loss of the thin film coated on the DPO is given by,

$$\phi_{\rm film} = \frac{G_{\rm sub}t_{\rm sub}}{3G_{\rm film}t_{\rm film}}(\phi_{\rm coated} - \phi_{\rm uncoated}). \tag{4}$$

The strain moduli (G) of the thin films were calculated using the Young's modulus (E) and Poisson's ratio (ν) from [6, 27, 28], and assumed to be temperature independent over the measured temperature range [29]. The elastic constants used are given in table 1.

Table 1. The elastic constants of Ti:GeO_2 systems were adopted from [6, 30] where the authors estimated values using the measured shift in the resonant mode frequencies after thin film deposition, and finite element modelling (FEM) analysis using COMSOL.

Ti concentration (%)	Annealing temperature (°C)	Young's modulus E (GPa)	Poission's ratio ν	Shear modulus $G = \frac{E}{2(1+\nu)}$ (GPa)
0 (Undoped GeO_2)	As-deposited	42.9±0.3	0.23 ±0.03	17.4 ±0.4
	500	43.3 ±0.8	0.29 ±0.04	16.8 ±0.6
26	As-deposited	57.1 ±0.6	0.31 ±0.04	21.8 ±0.7
	600	59.5 ±0.7	0.39 ±0.03	21.4 ±0.5
44	400	68.6 ±1.3	0.31 ±0.03	26.2 ±0.8
	500	66.1 ±1.3	0.31 ±0.03	25.2 ±0.8
	600	75.0 ±1.3	0.31 ±0.03	28.6 ±0.8

All the DPOs used in this study were fabricated in a single batch and one uncoated DPO was used as a control sample. Thin films ∼500 nm in thickness of GeO_2 and Ti:GeO_2 (26% and 44% (cation ratio) Ti were deposited using ion-beam sputtering, described in detail in [6, 7]. Temperature-dependent mechanical loss measurements were carried out on each of the coatings in an as-deposited (no annealing) and post-deposition annealed state at various temperatures. Annealing was carried out at 500°C or 600°C for 6 hrs in air with a heating and cooling ramp rate of 3°C per minute. Coatings with a similar doping concentration were deposited simultaneously on silicon wafers for grazing-incidence X-ray diffraction (GIXRD) characterization, and it was determined that all Ti-doped thin-films remain amorphous upon annealing up to 600°C and undoped GeO_2 remains amorphous up to 500°C.

3. Results and discussion

Figure 2(a) shows the temperature-dependent mechanical loss of an uncoated DPO, during cool-down to 70 K and reclamping it to the sample mount to test reproducibility of the results. The measured values of mechanical loss are observed to be reproducible within 2% which is similar to that previously reported by White *et al* in [31]. Figure 2(b) shows a representative plot of the temperature-dependent mechanical loss measured from a coated and uncoated DPO from 10 K to room temperature. We intermittently observed a kink at ∼ 30 K in the measured

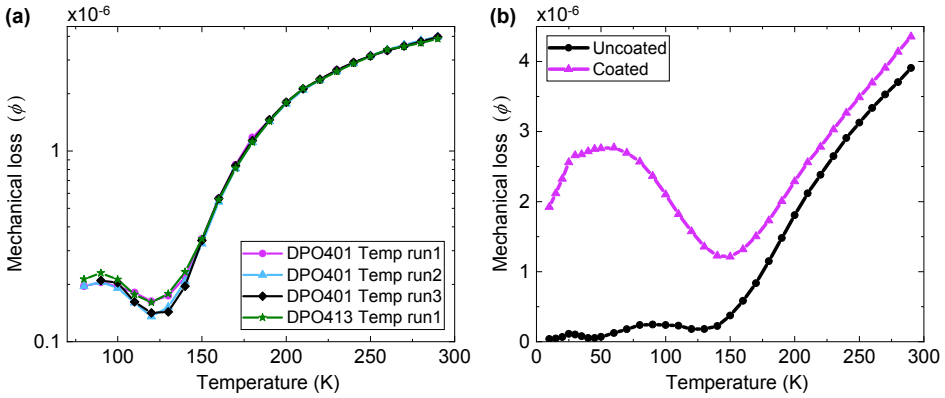

Figure 2. Temperature dependent mechanical loss of DPOs: (a) measured on an uncoated sample DPO401 after unclamping and reclamping to the sample mount, and another uncoated DPO413, demonstrating measurement reproducibility (plotted in a log scale to highlight the small changes observed between temperature runs and DPOs); and (b) from an uncoated control-sample and a coated samples with 44% Ti:GeO_2.

mechanical loss, which arose due to unwanted coupling of the resonator with the clamp. Subsequent experiments in reclamping the DPOs using epoxy eliminated this 30 K kink. Due to sequential annealing of the samples, it was not possible to repeat the measurements to obtain data without the 30 K kink. Any conclusions or trends drawn from the coating mechanical loss data presented in this work are independent from the observation of the 30 K kink, and as such it can be disregarded.

Figure 3 shows the temperature-dependent coating mechanical loss of as-deposited and annealed amorphous thin films of GeO_2 and Ti:GeO_2 thin films. The data presented in the gray shaded temperature regime above $\sim$150 K should be considered qualitative due to thermoelastic effects which preclude accurate evaluation of the mechanical loss; below 150 K thermoelastic effects are negligible [32]. Despite the ambiguity in absolute values of measured loss at room temperature due to thermoelastic effects, the trend observed for all films show that the mechanical loss near room temperature decreases with increasing annealing temperature, which is consistent with room temperature GeNS measurements on Ti:GeO_2 films deposited on silica disks [6]. This annealing phenomenon has been observed in multiple amorphous oxides and has been attributed to the redistribution of the atomic structure, with a decrease in the fraction of ES and CS polyhedra [16]. At temperatures below 150 K, the mechanical loss

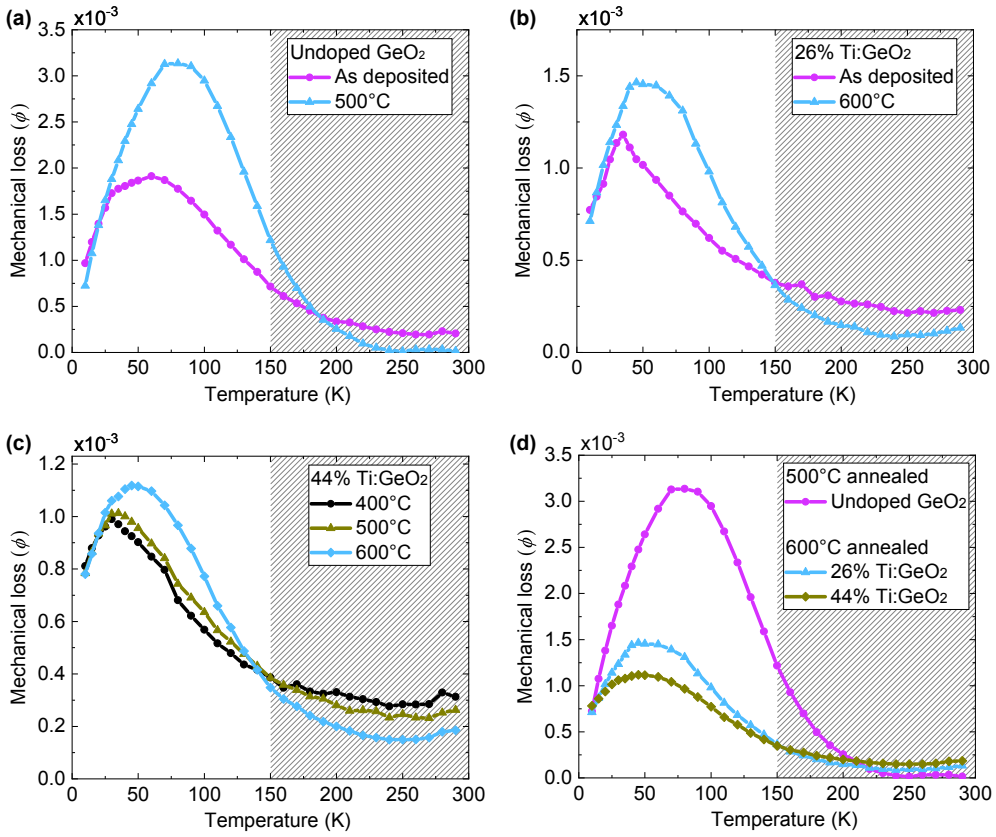

Figure 3. Temperature-dependent coating mechanical loss of as-deposited and annealed thin films of: (a) undoped GeO_2, (b) 26% Ti:GeO_2, (c) 44% Ti:GeO_2, and (d) comparison of annealed samples at different Ti-doping concentrations. The data above 150 K is shown as shaded region because this is where thermoelastic contribution to loss becomes significant and mechanical loss data is only qualitative.

of GeO_2 as well as Ti:GeO_2 increases as the annealing temperature increases. All films show a broad low-temperature peak below 100 K, as is typical in amorphous oxides [17, 33–35], which narrows and shifts towards higher temperature upon increasing annealing temperature.

Figure 3(d) shows the mechanical loss of GeO_2 and Ti:GeO_2 coatings annealed at the maximum temperature at which they remain amorphous, which is 500°C for GeO_2 and 600°C for Ti:GeO_2. The trend shown by the room temperature mechanical loss of Ti:GeO_2 films as a function of doping concentration is consistent with the trend observed in GeNS measurements by Vajente *et al* [6]. At room temperature, undoped GeO_2 has the lowest room temperature mechanical loss of $\sim 0.5 \times 10^{-4}$ which increases to $\sim 1.5 \times 10^{-4}$ when doped with 44% Ti [6]. This trend is consistent with the empirical correlation of the density of ES and FS polyhedra with the mechanical loss observed in [16], as Ti-doping increases the density of ES and FS polyhedra in GeO_2. The benefit of using Ti-doping in GeO_2 lies only in increasing the refractive index to reduce the layer-pairs required in an high-reflective stack. The magnitude of the low-temperature loss peak decreases and shifts to lower temperatures with increased Ti-doping.

A similar effect of reducing the low temperature loss with increasing Ti-doping concentration is observed in Ti:Ta_2O_5 [36]. However, room temperature loss shows the opposite trend, where Ti-doping reduces the mechanical loss in Ti:Ta_2O_5 [37] and increases in Ti:GeO_2. The origin of this difference in behavior between GeO_2 and Ta_2O_5-based films may be related to the difference in polyhedral connections between undoped-GeO_2 vs Ta_2O_5, where GeO_2 is entirely corner-shared and Ta_2O_5 has a high density of ES and FS polyhedra. Further structural characterisation to elucidate this difference in behavior will be the subject of future research.

Figure 4 shows the mechanical loss of bulk and thin film SiO_2 and GeO_2. Both the thin films of SiO_2 as well as GeO_2 were annealed at 600 °C for 24 hrs and 6 hrs respectively. The low-temperature peak centered at $\sim$35 K in bulk SiO_2 [38] has been shifted to lower temperature $\sim$20 K in the thin film [11]. A similar trend is observed in GeO_2, with the low-temperature peak centered at $\sim$120 K of bulk GeO_2 [17] shifted to lower temperature at $\sim$60 K in the thin film. Additionally, in SiO_2 and GeO_2, as observed in other amorphous oxides [10, 16], the mechanical loss increases at low temperature and decreases at room temperature upon annealing (prior to crystallization). In both SiO_2 and GeO_2, the room

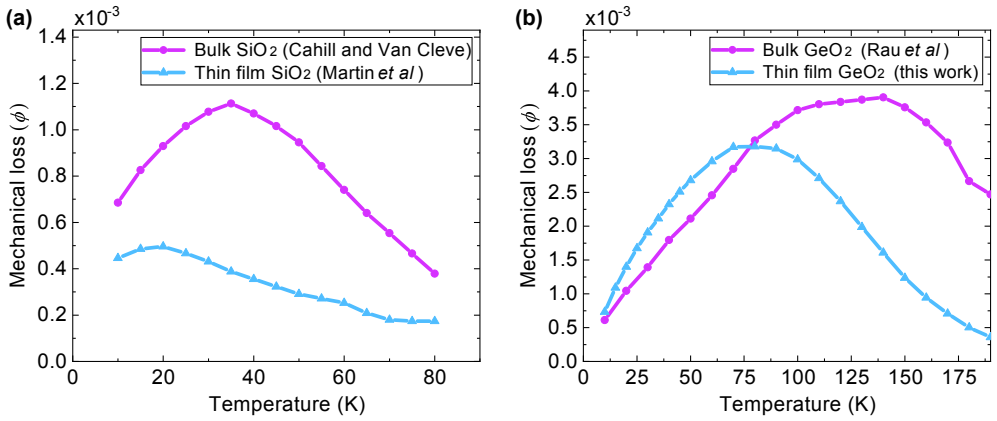

Figure 4. Temperature-dependent mechanical loss of bulk and thin films of (a) SiO_2 and (b) GeO_2. Bulk and thin film loss data for SiO_2 is obtained from [38] and [11], respectively. Bulk data for GeO_2 is obtained from [17].

temperature mechanical loss is higher in the thin films compared to the bulk, and is lower at cryogenic temperatures.

The structural origin of the behaviour between the bulk and thin film mechanical loss is not well understood. A recent study of Raman spectra from sputtered SiO_2 has indicated that thin films, when compared to bulk material, have higher concentration of three-membered rings and smaller inter-tetrahedral bond-angles [39]. A study by Granata *et al.* has shown that mechanical loss is correlated with density of three-membered rings of Si-O_4 tetrahedral units [40]. Raman studies in GeO_2 by Yang et al. have also found evidence of three-membered rings and have shown that the density of these rings could be influenced by changing the deposition temperature [7]. Furthermore, atomic modeling on the effects of annealing has shown that the concentration of smaller rings, including three-membered rings, decreases upon annealing [41]. These small rings could be responsible for the mechanical loss at room temperature, as the bulk material has a lower concentration of small rings which correlates with the lower mechanical loss observed when compared to thin films. Damart and Rodney have suggested, based on studies of TLS in SiO_2, that the low temperature mechanical loss arises from the coordinated displacement of oxygen atoms, without bond-breaking, in several SiO_4 polyhedra connected by chains or rings [42]. Billman *et al* made a similar prediction, suggesting it involves the rotation of oxygen atoms in several polyhedra by roughly 15° [14], however they also suggest it may involve coordination changes which implies bond-breaking and is in contradiction with Damart and Rodney's observations.

Frequency-dependent mechanical loss measurements on these systems, and extraction of the barrier height and relaxation rate distributions for the thermally activated transitions in the TLS responsible for these losses would provide useful data for testing structural models of these materials [17, 33, 34], and will be the subject of future research. Additionally, recent studies have shown an unexplained discrepancy between direct thermal noise measurements and extrapolated thermal noise from ring-down measurements [43]. Understanding the origin of this discrepancy will be important in fully understanding thermal noise and finding coating solutions for future GW detectors.

4. Conclusion

The temperature-dependent mechanical loss of Ti:GeO_2 coatings was studied as both a function of Ti-doping and post-deposition annealing. Undoped germania has a wide cryogenic loss peak centering at 60 K, with the peak value of $\sim 3.2 \times 10^{-3}$ which decreases to $\sim 1.2 \times 10^{-3}$ as the TiO_2 concentration increases to 44%. In addition to decreasing the height of the cryogenic loss peak, TiO_2 doping increases the width of this peak and shifts the peak position towards lower temperature. Post-deposition annealing reduces the room-temperature mechanical loss of GeO_2 and Ti:GeO_2 and increases its mechanical loss below 100 K, and also shifts the low-temperature peak to higher temperatures.

The comparison of the temperature-dependent loss for bulk and thin-film amorphous SiO_2 and GeO_2 shows similar features. Mechanical loss at cryogenic temperatures in both of their bulk forms was found to be higher than that of their corresponding thin films. Atomic structure studies involving Raman measurements and TLS modeling suggest that TLS involving small rings could give rise to room temperature loss whereas low temperature loss could involve the coordinated displacement of oxygen atoms across several SiO_4 polyhedra.

Using DPOs as resonators allowed us to study the mechanical loss at only one mode at around 5.65 kHz, which precluded frequency-dependent measurements. Frequency-dependent measurements as a function of temperature would enable a more detailed investigation of the dissipation mechanisms, and is the subject of future research.

Acknowledgements

The authors would like to acknowledge the valuable help and discussions with Matthew Abernathy, Tom Metcalf, and Xiao Liu at the Naval Research Laboratory, USA. This work was supported by the LSC Center for Coatings Research, jointly funded by the National Science Foundation (NSF) and the Gordon and Betty Moore Foundation (GBMF). In particular, we are grateful for support through NSF awards PHY-2011571 and PHY-2011706, and GBMF Grant No. 6793. Part of this work was performed at the Stanford Nanofabrication Facility (SNF) and the Stanford Nano Shared Facilities (SNSF), supported by the NSF under awards ECCS-1542152 and ECCS-2026822, respectively. Martin and Tait acknowledge support from STFC under ST/N005422/1 and ST/V005634/1. This paper has LIGO document No. P2300122.

References

[1] J Aasi et al. Advanced ligo. *Classical and quantum gravity*, 32(7):074001, 2015.

[2] F Acernese et al. Advanced virgo: a second-generation interferometric gravitational wave detector. *Classical and Quantum Gravity*, 32(2):024001, 2014.

[3] A Amato et al. Optical properties of high-quality oxide coating materials used in gravitational-wave advanced detectors. *Journal of Physics: Materials*, 2(3):035004, 2019.

[4] M Granata et al. Mechanical loss in state-of-the-art amorphous optical coatings. *Physical Review D*, 93(1):012007, 2016.

[5] M Granata et al. Amorphous optical coatings of present gravitational-wave interferometers. *Classical and Quantum Gravity*, 37(9):095004, 2020.

[6] G Vajente et al. Low mechanical loss TiO_2: GeO_2 coatings for reduced thermal noise in gravitational wave interferometers. *Physical Review Letters*, 127(7):071101, 2021.

[7] L Yang et al. Enhanced medium-range order in vapor-deposited germania glasses at elevated temperatures. *Science advances*, 7(37):eabh1117, 2021.

[8] R X Adhikari et al. A cryogenic silicon interferometer for gravitational-wave detection. *Classical and Quantum Gravity*, 37(16):165003, 2020.

[9] M Abernathy et al. Einstein gravitational wave telescope conceptual design study. 2011.

[10] I W Martin et al. Effect of heat treatment on mechanical dissipation in Ta_2O_5 coatings. *Classical and Quantum Gravity*, 27(22):225020, 2010.

[11] I W Martin et al. Low temperature mechanical dissipation of an ion-beam sputtered silica film. *Classical and Quantum Gravity*, 31(3):035019, 2014.

[12] J Lu and Y Kuo. Hafnium-doped tantalum oxide high-k dielectrics with sub-2 nm equivalent oxide thickness. *Applied Physics Letters*, 87(23):232906, 2005.

[13] J Trinastic et al. Molecular dynamics modeling of mechanical loss in amorphous tantala and titania-doped tantala. *Physical Review B*, 93(1):014105, 2016.

[14] C R Billman et al. Origin of the second peak in the mechanical loss function of amorphous silica. *Physical Review B*, 95(1):014109, 2017.

[15] Matthieu Micoulaut, L Cormier, and GS Henderson. The structure of amorphous, crystalline and liquid geo2. *Journal of Physics: Condensed Matter*, 18(45):R753, 2006.

[16] K Prasai et al. High precision detection of change in intermediate range order of amorphous zirconia-doped tantala thin films due to annealing. *Physical review letters*, 123(4):045501, 2019.

[17] S Rau et al. Acoustic properties of oxide glasses at low temperatures. *Physical Review B*, 52(10):7179, 1995.

[18] I Martin et al. Measurements of a low-temperature mechanical dissipation peak in a single layer of ta2o5 doped with tio2. *Classical and Quantum gravity*, 25(5):055005, 2008.

[19] S Reid et al. Mechanical dissipation in silicon flexures. *Physics Letters A*, 351(4-5):205–211, 2006.

[20] E Cesarini et al. A "gentle" nodal suspension for measurements of the acoustic attenuation in materials. *Review of Scientific Instruments*, 80(5):053904, 2009.

[21] G Vajente et al. A high throughput instrument to measure mechanical losses in thin film coatings. *Review of Scientific Instruments*, 88(7):073901, 2017.

[22] C L Spiel, R O Pohl, and A T Zehnder. Normal modes of a si (100) double-paddle oscillator. *Review of Scientific Instruments*, 72(2):1482–1491, 2001.

[23] T H Metcalf. *Elastic properties, annealing, and vapor pressure of neon and argon films*. Cornell University, 2002.

[24] H Wei and J Pomeroy. Application of the double paddle oscillator for quantifying environmental, surface mass variation. *Metrologia*, 53(2):869, 2016.

[25] X Liu et al. On the modes and loss mechanisms of a high q mechanical oscillator. *Applied Physics Letters*, 78(10):1346–1348, 2001.

[26] T H Metcalf, X Liu, and M R Abernathy. Improving the mechanical quality factor of ultra-low-loss silicon resonators. *Journal of Applied Physics*, 123(23):235105, 2018.

[27] G Vajente et al. Update on titania-doped germania. *https://dcc.ligo.org/LIGO-G2100386-v1*, LIGO Document- G2100386-v1.

[28] G Vajente et al. Update on a+ coatings. *https://dcc.ligo.org/LIGO-G2000576-v2*, LIGO Document- G2000576-v2.

[29] S Spinner and G W Cleek. Temperature dependence of young's modulus of vitreous germania and silica. *Journal of Applied Physics*, 31(8):1407–1410, 1960.

[30] M Fazio et al. Comprehensive study of amorphous metal oxide and Ta_2O_5-based mixed oxide coatings for gravitational-wave detectors. *Physical Review D*, 105(10):102008, 2022.

[31] B E White and R O Pohl. Elastic properties of thin films. *MRS Online Proceedings Library (OPL)*, 356, 1994.

[32] B H Houston et al. Thermoelastic loss in microscale oscillators. *Applied Physics Letters*, 80(7):1300–1302, 2002.

[33] J Classen et al. Low frequency acoustic and dielectric measurements on glasses. *Annalen der Physik*, 506(5):315–335, 1994.

[34] P Neu and A Würger. Relaxation due to incoherent tunnelling in dielectric glasses. *EPL (Europhysics Letters)*, 27(6):457, 1994.

[35] K A Topp and David G Cahill. Elastic properties of several amorphous solids and disordered crystals below 100 k. *Zeitschrift für Physik B Condensed Matter*, 101(2):235–245, 1996.

[36] I W Martin et al. Comparison of the temperature dependence of the mechanical dissipation in thin films of Ta_2O_5 and Ta_2O_5 doped with TiO_2. *Classical and Quantum Gravity*, 26(15):155012, 2009.

[37] G M Harry et al. Titania-doped tantala/silica coatings for gravitational-wave detection. *Classical and Quantum Gravity*, 24(2):405, 2006.

[38] D G Cahill and J E Van Cleve. Torsional oscillator for internal friction data at 100 khz. *Review of scientific instruments*, 60(8):2706–2710, 1989.

[39] S B Khemis et al. Structural analysis of sputtered amorphous silica thin films: A raman spectroscopy investigation. *Thin Solid Films*, 733:138811, 2021.

[40] M Granata et al. Correlated evolution of structure and mechanical loss of a sputtered silica film. *Physical Review Materials*, 2(5):053607, 2018.

[41] K Prasai et al. Annealing-induced changes in the atomic structure of amorphous silica, germania, and tantala using accelerated molecular dynamics. *physica status solidi (b)*, 258(9):2000519, 2021.

[42] T Damart and D Rodney. Atomistic study of two-level systems in amorphous silica. *Physical Review B*, 97(1):014201, 2018.

[43] A Amato et al. Optical and mechanical properties of ion-beam-sputtered Nb_2O_5 and TiO_2-Nb_2O_5 thin films for gravitational-wave interferometers and an improved measurement of coating thermal noise in advanced ligo. *Physical Review D*, 103(7):072001, 2021.